

# Correlating galaxy shapes and initial conditions: observational study

Pavel Motloch,<sup>1</sup> Ue-Li Pen,<sup>1,2,3,4,5,6</sup> and Hao-Ran Yu<sup>7</sup>

<sup>1</sup>Canadian Institute for Theoretical Astrophysics, University of Toronto, M5S 3H8, ON, Canada

<sup>2</sup>Department of Physics, University of Toronto, 60 St. George Street, Toronto, ON M5S 1A7, Canada

<sup>3</sup>Institute of Astronomy and Astrophysics, Academia Sinica,

Astronomy-Mathematics Building, No. 1, Section 4, Roosevelt Road, Taipei 10617, Taiwan

<sup>4</sup>Perimeter Institute for Theoretical Physics, Waterloo, N2L 2Y5, ON, Canada

<sup>5</sup>Canadian Institute for Advanced Research, CIFAR Program in Gravitation and Cosmology, Toronto, M5G 1Z8, ON, Canada

<sup>6</sup>Dunlap Institute for Astronomy and Astrophysics, University of Toronto, M5S 3H4, ON, Canada

<sup>7</sup>Department of Astronomy, Xiamen University, Xiamen, Fujian 361005, China

We find that galaxy angular momenta determined from shapes of spiral galaxies correlate with the initial tidal field in the galaxy’s neighborhood. Explicitly, we find that the galaxies tend to be preferentially face on (edge on) oriented when the major (minor) axis of the initial tidal field is aligned with the line of sight. Because tidal-torque theory predicts vanishing of this kind of signal, the observed correlation suggests non-linear origin. This correlation is statistically significant even after considering the number of observables investigated. Our result provides motivation for considering galaxy shape information in the efforts aiming to reconstruct initial conditions in the Universe.

## I. INTRODUCTION

Galaxy surveys have been instrumental in enhancing our understanding of the Universe [1–4]. Beyond the traditional analyses, it is useful to think about how to extract additional information from the large number of galaxies that will be discovered in the following years [5, 6].

One of the suggestions has been using measurements of galaxy angular momenta, that can extend our understanding of physics at megaparsec scales [7–9]. Such measurements can aid with reconstruction of the initial conditions (ICs) in the Universe [7, 8] and help to constrain neutrino masses [10], primordial gravitational waves [11], primordial non-Gaussianity [12] and chirality violations in the early Universe [9]. Better knowledge of initial matter distribution in the local volume would also aid studies of galaxy formation.

In our current understanding, the dark matter haloes acquire angular momenta from the inhomogeneous tidal field that torques the non-spherical protohalo early on [13–17]. At late times, interactions with the nearby large scale structure notably complicate the picture [16–37].

Despite these late time effects, it turns out that the *direction* of the halo angular momentum retains a significant amount of the initial information [9]. Naturally, we can not directly measure angular momenta of dark matter haloes. Fortunately, spins<sup>\*1</sup> of galaxies tend to be correlated with spins of their dark matter haloes [38, 39], and so there is a potential to use measurements of galaxy spins to probe the initial conditions in the local Universe.

It seems that the *amplitude* of the dark matter halo’s angular momentum also retains information about the

initial conditions [40] (but see [16, 39]). However, in this work we only consider the angular momenta directions, especially given the experimental cost involved in determining the amplitudes of galaxy angular momenta.

The prospect that measurements of galaxy spins might help with the reconstruction of the initial conditions in the Universe requires an observational verification. We made a first step in this direction in [41], where we found a correlation between the galaxy spins of a sample of about 15000 galaxies and initial conditions reconstructed from positions of a larger sample of galaxies [42]. Unfortunately, due to the limited number of galaxies we could only confirm this correlation with a  $\sim 3\sigma$  confidence. To achieve this result, we combined a set of galaxies for which integral field spectroscopy data is available with a set of spiral galaxies with known senses of rotation of their spiral arms.

At least in principle we have access to a significantly larger dataset of galaxy spins. Assuming that each spiral galaxy forms a thin disk with its spin pointing perpendicularly to the plane of the disk, we can utilize shape measurements of spiral galaxies to determine their spins up to a so-called four-fold degeneracy (see below) [7]. Shape measurements of spiral galaxies, as a proxy for their spins, are thus potentially useable as an additional handle on the initial conditions of the Universe. In this paper we investigate to what extent such a proposition is viable by studying correlations between galaxy spin components determined solely from galaxy shapes and observables derived from the initial density field as measured using a traditional reconstruction technique. In contrast with [41], we trade a somewhat lower signal per galaxy (due to the four-fold degeneracy) for a larger number of galaxies. Unlike the previous studies such as [43], we study correlations of galaxy shapes with observables derived from *initial*, not late time, density field.

This paper is organized as follows: In § II we describe how to determine galaxy spins from the galaxy shape measurements and discuss the four-fold degeneracy

<sup>\*1</sup> As a shorthand, here and in what follows we use “spin” to specifically only refer to the direction of the angular momentum of a halo/galaxy, ignoring its amplitude.

acy. Then we explain how we quantify correlations between galaxy spins and the initial conditions and list the observables built from the initial conditions we consider in this work. In § III we introduce the data used and in § IV we present our results. We conclude with discussion in § V.

We use indices  $i, j, k, l$  to denote components of vectors and tensors in three dimensions.

## II. THEORY

In this section we introduce the thin disk approximation that we use to connect measurements of galaxy shapes and their angular momenta. Then we describe how we quantify correlations between galaxy spins and various observables built from the initial conditions, before listing all such observables considered in this work.

### A. Spins from shapes

Measuring the full 3D vector of galaxy angular momentum requires integral field spectroscopy, which is experimentally costly and can at the present only be obtained for several thousands of galaxies [44, 45]. Using an approximation in which spiral galaxies are considered to be thin disks allows us to use images of spiral galaxies to infer information about their angular momenta [23, 43]. Currently, tens of thousands of such images are available.

In this thin-disk approximation, matter is assumed to be circling around the galaxy center in the plane of the disk, implying that the galaxy angular momentum vector is perpendicular to the plane of the galaxy. This plane can be, up to a two-fold degeneracy, determined from the position angle  $\alpha$  and axis ratio  $\mathcal{R}$  of the galaxy image. Additional two-fold degeneracy then arises because from  $\alpha$  and  $\mathcal{R}$  alone we are unable to determine whether the galaxy spin points towards or away from the observer.

The unit spin vector of such a galaxy in the local spherical coordinate frame  $(L_r, L_\theta, L_\phi)$  can be determined through [46]

$$\begin{aligned} |L_r| &= \mathcal{R} \\ L_\theta/L_\phi &= \tan \alpha, \end{aligned} \quad (1)$$

where the four-fold degeneracy prevents us from determining the signs of  $L_r$  and  $L_\theta$  (and thus  $L_\phi$ ) from the galaxy image alone.

In the equatorial Cartesian coordinates, the unit spin vector can be then determined from the right ascension and declination of the galaxy through [43]

$$\vec{L} = \vec{L}_R + \vec{L}_T, \quad (2)$$

where we defined

$$\begin{aligned} \vec{L}_R &\propto L_r (\sin \theta \cos \phi, \sin \theta \sin \phi, \cos \theta) \\ \vec{L}_T &\propto L_\theta (\cos \theta \cos \phi, \cos \theta \sin \phi, -\sin \theta) \\ &\quad + L_\phi (-\sin \phi, \cos \phi, 0) \end{aligned} \quad (3)$$

and  $\theta = \pi/2 - \text{DEC}$  and  $\phi = \text{RA}$ . Because of the four-fold degeneracy, signs of  $\vec{L}_{R,T}$  are ambiguous. Notice that in general neither of the vectors  $\vec{L}_{R,T}$  has unit norm.

By default we consider spiral galaxies to be infinitely thin disks and use (1). To test for systematic effect of this assumption, we also consider non-zero intrinsic flatness  $p$  of the spiral galaxies, where we replace  $\mathcal{R}$  in (1) with

$$\mathcal{R} \rightarrow \sqrt{\frac{\max(\mathcal{R}^2 - p^2, 0)}{1 - p^2}}. \quad (4)$$

Experimentally,  $p$  of spiral galaxies has been measured to be  $\sim 0.1 - 0.2$  [47].

### B. Quantifying correlations

In this section we give an overview of how we quantify correlations between measurements of galaxy spins as represented by  $\vec{L}_{R,T}$  and the initial conditions. In all cases, the initial conditions are represented by either a vector  $V_i$  or a rank-two tensor  $M_{ij}$  constructed from the second derivatives of the initial density  $\rho_{\text{ini}}$ , gravitational potential  $\phi_{\text{ini}}$ , or both.

Considering first the rank-two variables of the form  $M_{ij}$ , we can form three scalar combinations

$$L_R M L_R \equiv \sum_{ij} L_{Ri} M_{ij} L_{Rj} \quad (5)$$

$$L_T M L_T \equiv \sum_{ij} L_{Ti} M_{ij} L_{Tj} \quad (6)$$

$$L_T M L_R \equiv \sum_{ij} L_{Ti} M_{ij} L_{Rj}, \quad (7)$$

where for future convenience we suppressed the index structure on the left hand side. Given the four-fold degeneracy in determining  $\vec{L}_T$  and  $\vec{L}_R$ , the last combination can not be evaluated using the shape data alone. On the other hand,  $L_R M L_R$  and  $L_T M L_T$  are invariant with respect to this degeneracy and can be used to study the correlations between galaxy spins and initial conditions.

With vector variables  $V_i$  the situation is slightly more complicated, as the naive combinations  $\vec{L}_{R,T} \cdot \vec{V}$  are again indeterminate due to the uncertainty in the sign of  $\vec{L}_{R,T}$ . We can form an invariant quantity by taking the absolute value of the scalar product,

$$|L_R V| \equiv \left| \sum_i L_{Ri} V_i \right| \quad (8)$$

$$|L_T V| \equiv \left| \sum_i L_{Ti} V_i \right|, \quad (9)$$

which can be used to study the correlation of  $\vec{L}_{R,T}$  with the initial conditions. Notice that more information is available when we are able to break the degeneracy [41].

For each variable  $\mathcal{V}$  of the form  $L_\alpha M L_\alpha$  or  $|L_\alpha V|$  with  $\alpha \in \{R, T\}$  we then evaluate the average  $\langle \mathcal{V} \rangle$  over the galaxies in our sample. To determine the probability of observing such  $\langle \mathcal{V} \rangle$  in case of uncorrelated spins  $\vec{L}_{R,T}$  and initial conditions (as represented by  $M_{ij}/V_i$ ), we calculate  $\mathcal{V}$  for many mock galaxy catalogs in which the galaxy positions are kept fixed but we randomly shuffle the parameters  $\alpha, \mathcal{R}$  that determine the galaxy spins  $\vec{L}_{R,T}$ . As a result, we get the mean and standard deviation  $\bar{\mathcal{V}}, \sigma_{\mathcal{V}}$  of this random mock distribution, which allows us to calculate the statistical significance of the detected excess correlation

$$S = \frac{|\langle \mathcal{V} \rangle - \bar{\mathcal{V}}|}{\sigma_{\mathcal{V}}}. \quad (10)$$

Notice it is incorrect to shuffle the vectors  $\vec{L}_{T,R}$  themselves.

### C. Functions of initial conditions

In this section we introduce variables  $M_{ij}, V_i$  we use to characterize the initial conditions and which we correlate with the galaxy spins described by  $\vec{L}_{R,T}$ .

It has been shown in both simulations [9] and observations [41] that galaxy spins correlate with the vector field  $\vec{L}^{\text{IC}}$  defined in terms of the smoothed initial density  $\rho_{\text{ini}}^r$  and gravitational potential  $\phi_{\text{ini}}^r$  as

$$L_i^{\text{IC}} = \sum_{jkl} \epsilon_{ijk} \partial_{jl} \phi_{\text{ini}}^r \partial_{lk} \rho_{\text{ini}}^r. \quad (11)$$

The superscript  $r$  symbolizes the fields have been smoothed on scale  $r \sim O(h^{-1} \text{Mpc})$ . The unit norm vector field  $\hat{L}^{\text{IC}} = \vec{L}^{\text{IC}}/|L^{\text{IC}}|$  is then the first observable built from the initial conditions we correlate with the galaxy spins.

It has long been understood that tidal field in the vicinity of a protohalo plays a crucial role in determining the halo's spin [15]. This motivates us to pick the unit traceless local shear tensor  $\hat{T}$  [8] as our second variable. It is built from the shear tensor, defined as

$$T_{ij} = \partial_{ij} \phi_{\text{ini}}^r, \quad (12)$$

by first subtracting the trace

$$\tilde{T}_{ij} = T_{ij} - \frac{\delta_{ij}}{3} \sum_k T_{kk} \quad (13)$$

and then normalizing

$$\hat{T}_{ij} = \frac{\tilde{T}_{ij}}{\sqrt{\sum_{ij} \tilde{T}_{ij}^2}}. \quad (14)$$

The tidal-torque theory [13–17] predicts that the correlation  $\langle L_\alpha \hat{T} L_\alpha \rangle$  should vanish [8]: Assuming Gaussian

initial conditions, initial perturbation  $\phi_{\text{ini}}$  and its reverse  $-\phi_{\text{ini}}$  are equally likely. However, the observable  $\langle L_\alpha \hat{T} L_\alpha \rangle$  is not invariant under the operation  $\phi_{\text{ini}} \rightarrow -\phi_{\text{ini}}$  as  $\hat{T}_{ij}$  changes sign but the quadratic form  $L_{\alpha,i} L_{\alpha,j}$  does not. Physically, tidal-torque theory predicts equal alignments of galaxy spins with major and minor principal axes of  $\hat{T}$ , which leads to cancellations in  $\langle L_\alpha \hat{T} L_\alpha \rangle$ . Because vanishing of  $\langle L_\alpha \hat{T} L_\alpha \rangle$  is a realistic possibility, we also consider correlations with the second power of  $\hat{T}$ .

One can expect similar sensitivity to the second derivative of the initial density field, which can serve as a proxy for the protohalo's moment of inertia [29, 41]. We thus also investigate correlations with first and second power of  $\hat{I}_{ij}$ , defined similarly to  $\hat{T}_{ij}$  but with  $\phi_{\text{ini}}^r$  in (12) replaced by  $\rho_{\text{ini}}^r$ .

Finally, tidal-torque theory provides theoretical arguments that the galaxy spins should preferentially orient with the intermediate principal axis  $\hat{L}_0^\phi$  of the shear tensor  $\hat{T}$  [7]. In the limit where the tensor  $\hat{I}$  can be used as a proxy for the protohalo moment of inertia, the same arguments can be used to justify expectation of correlation of galaxy spins with the intermediate principal axis  $\hat{L}_0^\rho$  of  $\hat{I}$ . The two unit vectors  $\hat{L}_0^{\phi,\rho}$  are then the last two observables built from the initial conditions that we consider in this work.

Overall, we study correlations with seven objects constructed from the initial conditions: four matrices  $\hat{T}, (\hat{T})^2, \hat{I}, (\hat{I})^2$  and three vectors  $\hat{L}_0^\phi, \hat{L}_0^\rho, \hat{L}^{\text{IC}}$ . We correlate them with either  $\vec{L}_R$  or  $\vec{L}_T$ , which leads to 14 combinations to study for each of the smoothing scales we consider. Because we talk about the initial conditions, all these variables are evaluated at the *Lagrangian* positions of the galaxies.

## III. DATA

In this section we present the data used in this work. We start by describing the initial conditions as reconstructed by the ELUCID collaboration and then introduce the data used to determine angular momenta and positions of galaxies.

### A. Initial conditions

The initial density field  $\rho_{\text{ini}}$  used in this work was obtained by the ELUCID collaboration, extended details about their methodology can be found in [42, 48].

They first created a catalog of galaxy groups from the Sloan Digital Sky Survey (SDSS) data [49] and then estimated mass of each group via a luminosity-based abundance matching. After correcting for peculiar velocities, they only retained groups in the Northern Galactic Cap, redshift range  $0.01 \leq z \leq 0.12$  and with masses above  $10^{12} M_\odot$ . The space was then tessellated according to

which galaxy group was the closest. Within the resulting sub-volumes, particles were placed randomly, in accordance with the expected density profile for halo of given mass. This particle distribution represents today’s density field.

In the second step of the reconstruction, ELUCID collaboration determined the best fit initial conditions by repeatedly running a Particle-Mesh (PM) dynamics code in a Hamiltonian Monte Carlo fashion. For each random set of initial conditions, the PM code was used to calculate the corresponding value of today’s density field. This density field was compared with that determined from the SDSS data and their relative closeness was quantified using a predefined measure. As the PM code is inaccurate on small scales, before comparison both density fields were smoothed on a scale of 4 Mpc/h. Iteratively probing the space of initial conditions then allowed ELUCID to find the initial conditions that best describe the local galaxy data.

From the best fit  $\rho_{\text{ini}}$ , we use the Poisson equation to calculate the initial gravitational potential  $\phi_{\text{ini}}$ .

In [41] we found that with Elucid ICs, galaxy spins are best predicted when smoothing the initial conditions with  $r \sim 3$  Mpc/h. In this work we consider this smoothing scale, together with  $r \sim 2$  Mpc/h and  $r \sim 4$  Mpc/h to allow for the possibility of a potentially different optimal smoothing scale for the observables studied here.

## B. Galaxy shapes

Galaxy data used in this work were obtained by SDSS [4, 44] and we downloaded them from CasJobs<sup>\*2</sup>. First we use the Galaxy Zoo classifications [50] to select only spiral galaxies. For each such galaxy we obtain its right ascension, declination, redshift, position angle and axis ratio. As our default combination, for the position angle and axis ratio we use results of the fit of the de Vaucouleurs profile to the galaxy images obtained using the green SDSS filter. For systematic checks we also investigate other choices. As in our previous work, we only consider galaxies for which the closest Elucid halo was at least  $10^{12} M_{\odot}$  to avoid regions with poorly determined ICs.

For each galaxy, we calculate the vectors  $\vec{L}_{R,T}$  according to (3). The redshift and sky position then allows us to find each galaxy’s three-dimensional Euclidian position. Using the simulation ran from the optimal ICs, we then find the galaxy’s inverse displacement, which we use to calculate the Lagrangian position of the galaxy.

Our fiducial catalog contains 50361 galaxies in the volume in which Elucid provides the initial conditions.

TABLE I. Significances  $S$  of excess correlations in terms of number of standard deviations.

	Smoothing scale $r$		
	$2 h^{-1}\text{Mpc}$	$3 h^{-1}\text{Mpc}$	$4 h^{-1}\text{Mpc}$
$L_R \hat{T} L_R$	5.5	6.4	6.6
$L_T \hat{T} L_T$	0.9	0.6	0.3
$L_R (\hat{T})^2 L_R$	4.8	4.0	2.9
$L_T (\hat{T})^2 L_T$	2.5	2.7	2.7
$L_R \hat{I} L_R$	1.3	3.0	4.4
$L_T \hat{I} L_T$	1.4	1.1	0.6
$L_R (\hat{I})^2 L_R$	0.9	1.9	3.3
$L_T (\hat{I})^2 L_T$	0.2	0.3	0.9
$ L_R L_0^{\phi} $	3.8	3.4	2.6
$ L_T L_0^{\phi} $	1.6	2.3	1.6
$ L_R L_0^{\beta} $	1.1	1.5	2.1
$ L_T L_0^{\beta} $	0.2	0.7	0.4
$ L_R L^{IC} $	2.3	2.8	2.2
$ L_T L^{IC} $	0.0	1.1	2.0

## IV. RESULTS

In Fig. 1 we show our main result - excess correlation between the galaxy spins  $\vec{L}_{R,T}$  inferred from the galaxy shapes and various observables built from the initial conditions. We summarize the detection significances  $S$  in Table I. To estimate the error bars, we shuffled  $\mathcal{R}$  and  $\alpha$  total of 40000 times, which is enough to converge the results to below 0.05 standard deviation.

The strongest correlation we find is with the tidal tensor  $\hat{T}$ , which is significant for all three investigated smoothing scales  $r$ . We also see strong excess correlation between the galaxy spins and  $(\hat{T})^2$  smoothed with  $r = 2 h^{-1}\text{Mpc}$  and  $r = 3 h^{-1}\text{Mpc}$  and  $\hat{I}$  smoothed with  $r = 4 h^{-1}\text{Mpc}$ . No other correlations reach  $4\sigma$  significance.

We perform several tests to check for systematics. First we repeat the calculations assuming all galaxies have intrinsic flatness  $p = 0.1$ . This does not lead to any significant change in the results and neither does assuming  $p = 0.2$ . As an alternative study of the effect of the galaxy thickness, we uniformly redistribute all  $\mathcal{R}$  in the interval  $[0, 1]$  while keeping their original ordering [8]. Simultaneously we perform the same procedure on  $\alpha$ . Typical detection significance after this “isotropizing” rearrangement increases slightly, and no significance decreases by more than  $\sim 0.1$  standard deviation. Similar situation repeats when we use axis ratios and position angles from fits to the images obtained with the red SDSS filter: overall increase of the significances, with decreases of no more than  $\sim 0.15$  standard deviations.

The most dramatic change is observed when we use

<sup>\*2</sup> <https://skyserver.sdss.org/CasJobs/>

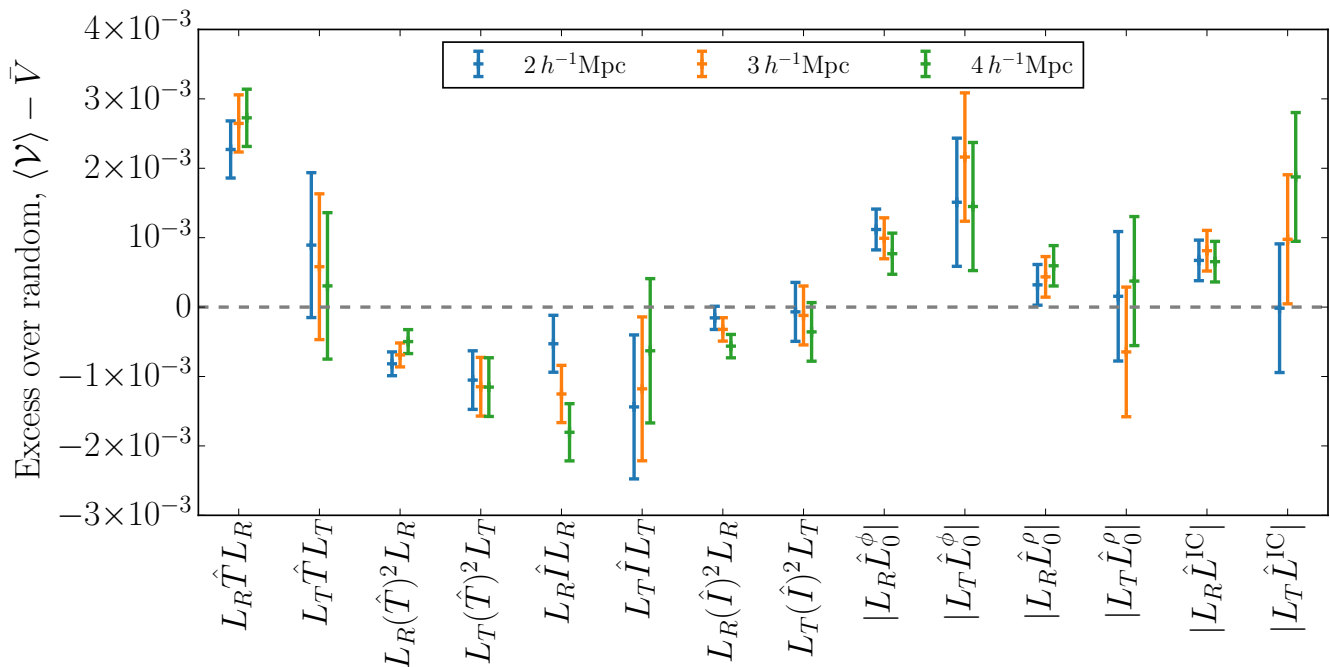


FIG. 1. Excess correlations of galaxy spins with various vectors and tensors derived from the initial conditions. Different colors represent different smoothing scales  $r$  used to calculate the vectors and tensors.

galaxy shapes obtained by fitting the exponential profile to the galaxy images, instead of the de Vaucouleurs one. The detection significance of  $L_R \hat{T} L_R$ , the observable we detect with the highest significance, drops by almost a full standard deviation and for the three smoothing scales ends up in the  $4.9 - 5.7 \sigma$  range. The other correlations are only changed within  $\pm 0.2\sigma$ .

We take  $5.7\sigma$  as a conservative estimate of the maximal discovered correlation. Because of the look-elsewhere effect, it is not possible to claim a  $5.7\sigma$  detection of correlation between the galaxy shapes and the initial condition given we investigate 42 different variables (listed in Table I). The overall detection significance can be bounded from below by calculating the probability of finding  $5.7\sigma$  or larger effect among 42 independent observations. It is

$$P = 1 - \left( \int_{-5.7}^{5.7} \frac{\exp(-x^2/2)}{\sqrt{2\pi}} dx \right)^{42} = 5 \times 10^{-7}, \quad (15)$$

which corresponds to  $\sim 5\sigma$ .

Correlations between the variables increase the detection significance, so to get a better estimate we take the covariance of the various observables  $\mathcal{V}$  into account. We estimate this covariance from the random reshuffling of  $\mathcal{R}$  and  $\alpha$  we used earlier to calculate  $\sigma_{\mathcal{V}}^2$ . We then simulate random draws from a Gaussian distribution with this covariance. We find that draws where any variable deviates by more than  $5.7\sigma$  from its expected value occur with probability  $2 \times 10^{-7}$ , which translates into our final estimate of the significance  $\sim 5.2\sigma$ . Had we started with the maximal local significance  $6.6\sigma$  we see when the results are based on fits of the de Vaucouleurs profile,

we would obtain a proportionally larger global detection significance.

Finally, we looked at the correlations in four bins in either redshift (Fig. 2) or halo mass (as estimated by ELUCID, Fig. 3) for the smoothing length  $r = 4 h^{-1} \text{Mpc}$ , where we see the most significant detection. We see mild trends in some of the observables, but given the large number of investigated data points it is expected to see dependencies just by pure chance and we do not pursue this issue further. We thus mainly use these splits as an additional systematic check. Given all redshift and halo mass bins lead to generally consistent results, we have checked that our results are not dominated by any outlier. These splits also serve as a rough check on the size of our error bars.

## V. DISCUSSION

In this work we studied correlations between directions of galaxy angular momenta determined from galaxy shapes (axis ratios and position angles) and various observables built from the initial density and gravitational potential.

We found a statistically significant correlation between the radial component of the galaxy spin  $\vec{L}_R$  and the tidal field in the vicinity of the protohalo (specifically the unit traceless shear tensor  $\hat{T}$ ). Physically this correspond to galaxies being preferentially oriented face on (edge on) in places where the major (minor) axis of the tidal field aligns with the line of sight. The detection was significant

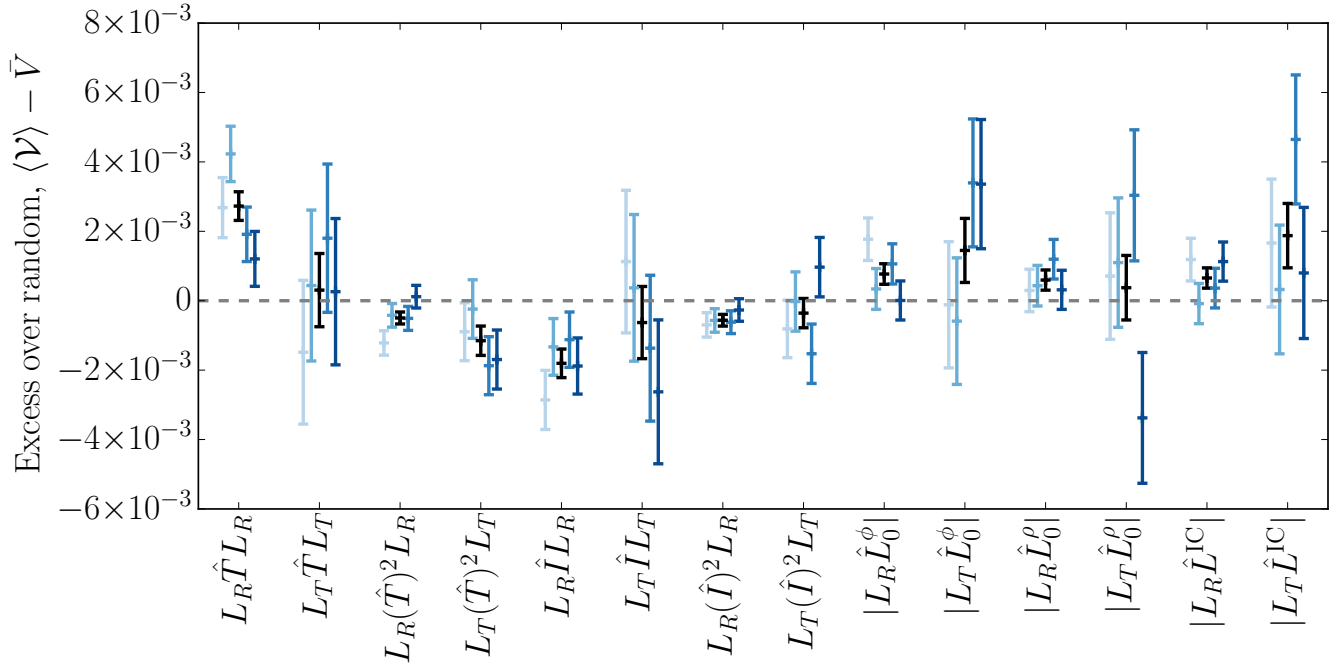


FIG. 2. Testing the redshift evolution. The black points correspond to the results obtained using all galaxies, already shown in Fig. 1. Each blue point represents results derived with a quarter of the galaxies, split based on their redshift. The darker the blue point, the further the galaxies are (i.e. the lightest/darkest blue points represent the results obtained using only the 25% closest/furthest galaxies). All with  $r = 4 h^{-1} \text{Mpc}$ .

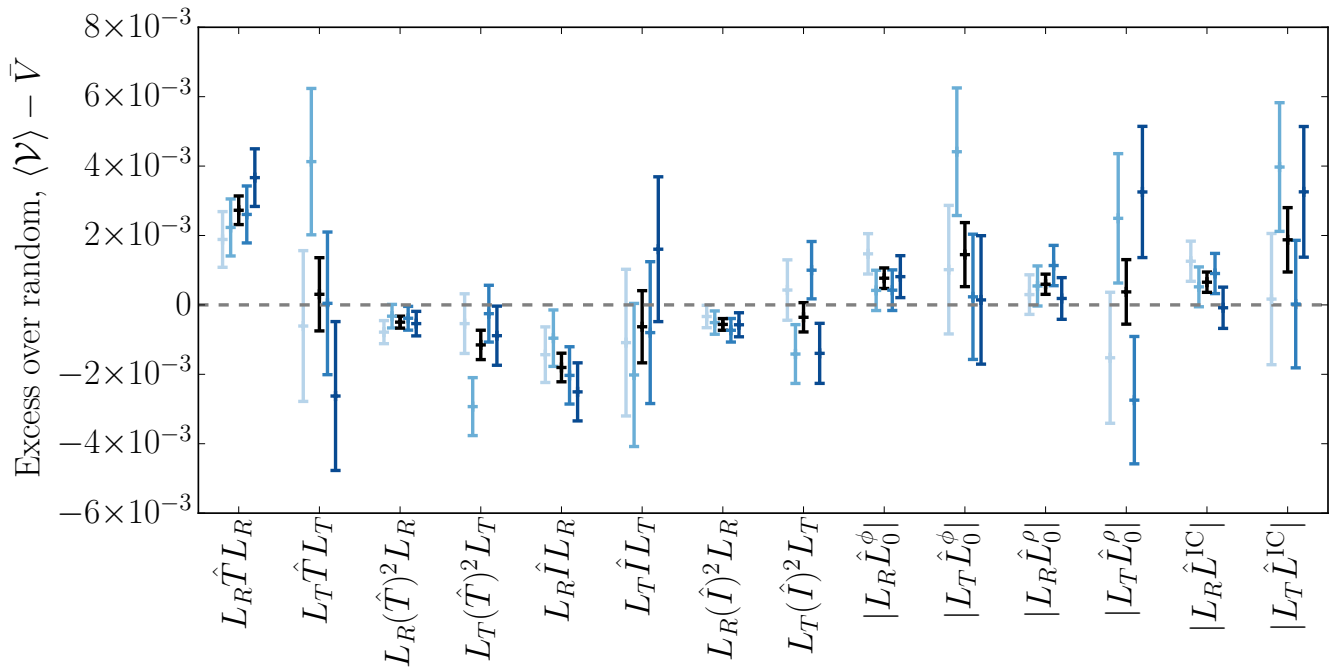


FIG. 3. Testing the halo mass dependence. As Fig. 2, only galaxies are split into bins according to the halo mass (as determined by ELUCID). Lighter blue represents galaxies in lighter haloes.

at the  $5.5\sigma - 6.6\sigma$  level when we use galaxy shape parameters determined from the de Vaucouleurs fit to the SDSS galaxy images, the largest significance was found when smoothing the initial conditions with  $r = 4h^{-1}\text{Mpc}$ . With shape parameters determined from the exponential fit to the galaxy images, the detection significance drops to  $4.9\sigma - 5.7\sigma$ . Considering the look-elsewhere effect, we estimate the global detection significance at  $5.2\sigma$ .

We explain above that the tidal-torque theory predicts vanishing  $\langle L_R \hat{T} L_R \rangle$ . As this theory is based on the first order perturbation theory described by the Zeldovich approximation, detection reported in this paper suggests we are detecting a non-perturbative effect. This complements earlier reports pointing out limitations of the tidal-torque theory (e.g. [16, 51]).

When smoothing with  $r = 4h^{-1}\text{Mpc}$ , we also find correlation with the unit traceless inertia tensor  $\hat{I}$ , with local significance of  $4.4\sigma$ . Interestingly, at about  $2.8\sigma$  significance we detect correlation with the spin galaxy proxy  $\hat{L}^{\text{IC}}$ . This is comparable to what was found in [41] with a smaller number of galaxies, though with access to additional information that allowed us to break the four-fold degeneracy.

In general, excess signals are compatible when using either  $\vec{L}_R$  or  $\vec{L}_T$ , galaxy spin vectors parallel and tangential to the line of sight. The error bars are always larger for correlations including  $\vec{L}_T$ , which is understandable given that the position angle  $\alpha$  acts as an additional source of uncertainty.

The initial conditions as provided by ELUCID are increasingly uncertain on smaller and smaller scales. It is unclear whether our detection is limited by this uncertainty, or by other factors, such as the late time evolution of the galaxy spins.

Overall, we have shown that galaxy shapes of spiral galaxies, explicitly the axis ratios of their images, provide additional information about the initial conditions. It is thus possible that including the galaxy shape measurements in the reconstruction efforts such as described in [48, 52–56] might improve the process of reconstruction of the initial conditions in the Universe, though this prospect warrants further investigation in simulations.

## ACKNOWLEDGMENTS

This work was supported by Natural Sciences and Engineering Research Council of Canada (NSERC) grant CITA 490888. P.M. was additionally supported by Vincent and Beatrice Tremaine Fellowship. U.-L.P. received additional support from Ontario Research Fund-research Excellence Program grant RE09-024, NSERC grants RGPIN-2019-067, 523638-201, CRDPJ 523638-2, Canadian Institute for Advanced Research grants FS21-146 and APPT, Canadian Foundation for Innovation grant IOF-33526, Simons Foundation grant 568354, Thoth Technology Inc., and the Alexander von Humboldt Foundation. H.-R.Y. additionally acknowledges support from National Natural Science Foundation of China grant 11903021.

- 
- [1] M. J. Geller and J. P. Huchra, *Science* **246**, 897 (1989).
  - [2] M. Colless *et al.*, (2003), arXiv:astro-ph/0306581.
  - [3] S. P. Driver *et al.*, *Mon. Not. Roy. Astron. Soc.* **413**, 971 (2011), arXiv:1009.0614 [astro-ph.CO].
  - [4] D. G. York *et al.* (SDSS), *Astron. J.* **120**, 1579 (2000).
  - [5] M. Levi *et al.* (DESI), (2013), arXiv:1308.0847 [astro-ph.CO].
  - [6] P. A. Abell *et al.* (LSST Science, LSST Project), (2009), arXiv:0912.0201 [astro-ph.IM].
  - [7] J. Lee and U.-L. Pen, *Astrophys. J.* **532**, L5 (2000).
  - [8] J. Lee and U.-L. Pen, *Astrophys. J.* **555**, 106 (2001).
  - [9] H.-R. Yu, P. Motloch, U.-L. Pen, Y. Yu, H. Wang, H. Mo, X. Yang, and Y. Jing, *Phys. Rev. Lett.* **124**, 101302 (2020).
  - [10] H.-R. Yu, U.-L. Pen, and X. Wang, *Phys. Rev.* **D99**, 123532 (2019).
  - [11] M. Biagetti and G. Orlando, *J. Cosmo. Astropart. Phys.* **07**, 005 (2020).
  - [12] F. Schmidt, N. E. Chisari, and C. Dvorkin, *J. Cosmo. Astropart. Phys.* **1510**, 032 (2015).
  - [13] P. Peebles, *Astrophys. J.* **155**, 393 (1969).
  - [14] A. G. Doroshkevich, *Astrophys. J.* **6**, 320 (1970).
  - [15] S. D. M. White, *Astrophys. J.* **286**, 38 (1984).
  - [16] C. Porciani, A. Dekel, and Y. Hoffman, *Mon. Not. R. Astron. Soc.* **332**, 325 (2002).
  - [17] C. Porciani, A. Dekel, and Y. Hoffman, *Mon. Not. R. Astron. Soc.* **332**, 339 (2002).
  - [18] A. Krolewski *et al.*, *Astrophys. J.* **876**, 52 (2019).
  - [19] D. DeFelippis, S. Genel, G. L. Bryan, and S. M. Fall, *Astrophys. J.* **841**, 16 (2017), arXiv:1703.03806 [astro-ph.GA].
  - [20] Y. Zhang *et al.*, *Astrophys. J.* **798**, 17 (2015).
  - [21] P. G. Veena, M. Cautun, R. van de Weygaert, E. Tempel, B. J. Jones, S. Rieder, and C. S. Frenk, *Mon. Not. R. Astron. Soc.* **481**, 414 (2018).
  - [22] P. Ganeshaiah Veena, M. Cautun, E. Tempel, R. van de Weygaert, and C. S. Frenk, *Mon. Not. R. Astron. Soc.* **487**, 1607 (2019).
  - [23] K. Kraljic, C. Duckworth, R. Tojeiro, S. Alam, D. Bizyaev, A.-M. Weijmans, N. F. Boardman, and R. R. Lane, *Mon. Not. Roy. Astron. Soc.* **504**, 4626 (2021), arXiv:2104.08275 [astro-ph.GA].
  - [24] K. Kraljic, R. Dave, and C. Pichon, *Mon. Not. Roy. Astron. Soc.* **493**, 362 (2020), arXiv:1906.01623 [astro-ph.GA].
  - [25] P. Wang and X. Kang, *Mon. Not. Roy. Astron. Soc.* **473**, 1562 (2018), arXiv:1709.07881 [astro-ph.CO].
  - [26] M. C. Neyrinck, M. A. Aragon-Calvo, B. Falck, A. S. Szalay, and J. Wang, *Open J. Astrophys.* **3**, 3 (2020), arXiv:1904.03201 [astro-ph.CO].

- [27] B. M. Schaefer, *Int. J. Mod. Phys. D* **18**, 173 (2009).
- [28] S. Codis, C. Pichon, J. Devriendt, A. Slyz, D. Pogosyan, Y. Dubois, and T. Sousbie, *Mon. Not. R. Astron. Soc.* **427**, 3320 (2012).
- [29] S. Codis, C. Pichon, and D. Pogosyan, *Mon. Not. R. Astron. Soc.* **452**, 3369 (2015).
- [30] C. Welker *et al.*, *Mon. Not. R. Astron. Soc.* **491**, 2864 (2020).
- [31] B. J. Jones, R. van de Weygaert, and M. A. Aragon-Calvo, *Mon. Not. R. Astron. Soc.* **408**, 897 (2010).
- [32] M. A. Aragon-Calvo, R. van de Weygaert, B. J. Jones, and J. van der Hulst, *Astrophys. J. Lett.* **655**, L5 (2007).
- [33] O. Hahn, C. Carollo, C. Porciani, and A. Dekel, *Mon. Not. R. Astron. Soc.* **381**, 41 (2007).
- [34] P. E. Bett and C. S. Frenk, *Mon. Not. R. Astron. Soc.* **420**, 3324 (2012).
- [35] P. E. Bett and C. S. Frenk, *Mon. Not. R. Astron. Soc.* **461**, 1338 (2016).
- [36] E. Tempel and N. I. Libeskind, *Astrophys. J. Lett.* **775**, L42 (2013).
- [37] P. Wang, Q. Guo, X. Kang, and N. I. Libeskind, *Astrophys. J.* **866**, 138 (2018).
- [38] A. F. Teklu *et al.*, *Astrophys. J.* **812**, 29 (2015).
- [39] F. Jiang *et al.*, *Mon. Not. R. Astron. Soc.* **488**, 4801 (2019).
- [40] Q. Wu, H.-R. Yu, S. Liao, and M. Du, *Phys. Rev. D* **103**, 063522 (2021), [arXiv:2011.03893 \[astro-ph.CO\]](https://arxiv.org/abs/2011.03893).
- [41] P. Motloch, H.-R. Yu, U.-L. Pen, and Y. Xie, *Nature Astron.* **5**, 283 (2021), [arXiv:2003.04800 \[astro-ph.CO\]](https://arxiv.org/abs/2003.04800).
- [42] H. Wang *et al.*, *Astrophys. J.* **831**, 164 (2016).
- [43] J. Lee and P. Erdogdu, *Astrophys. J.* **671**, 1248 (2007).
- [44] D. S. Aguado *et al.*, *Astrophys. J. Suppl.* **240**, 23 (2019).
- [45] N. Scott *et al.*, *Mon. Not. R. Astron. Soc.* **481**, 2299 (2018).
- [46] U.-L. Pen, J. Lee, and U. Seljak, *Astrophys. J. Lett.* **543**, L107 (2000), [arXiv:astro-ph/0006118](https://arxiv.org/abs/astro-ph/0006118).
- [47] M. P. Haynes and R. Giovanelli, *Astronomical Journal* **89**, 758 (1984).
- [48] H. Wang, H. J. Mo, X. Yang, Y. P. Jing, and W. P. Lin, *Astrophys. J.* **794**, 94 (2014).
- [49] X. Yang *et al.*, *Astrophys. J.* **671**, 153 (2007).
- [50] C. J. Lintott *et al.*, *Mon. Not. R. Astron. Soc.* **389**, 1179 (2008).
- [51] L. Hui and J. Zhang, (2002), [arXiv:astro-ph/0205512](https://arxiv.org/abs/astro-ph/0205512).
- [52] J. Jasche and B. D. Wandelt, *Mon. Not. R. Astron. Soc.* **432**, 894 (2013).
- [53] H.-M. Zhu, Y. Yu, U.-L. Pen, X. Chen, and H.-R. Yu, *Phys. Rev.* **D96**, 123502 (2017).
- [54] M. Schmittfull, T. Baldauf, and M. Zaldarriaga, *Phys. Rev.* **D96**, 023505 (2017).
- [55] R. Hada and D. J. Eisenstein, *Mon. Not. R. Astron. Soc.* **478**, 1866 (2018).
- [56] H.-M. Zhu, M. White, S. Ferraro, and E. Schaan, *Mon. Not. R. Astron. Soc.* **494**, 4244 (2020).